

³He Transverse (e,e') Response Function in the Quasielastic Region

V.D. Efros¹, W. Leidemann^{2,a}, G. Orlandini², and E.L. Tomusiak³

¹ Russian Research Centre "Kurchatov Institute", 123182 Moscow, Russia

² Dipartimento di Fisica, Università di Trento, and Istituto Nazionale di Fisica Nucleare, Gruppo Collegato di Trento, I-38050 Povo, Italy

³ Department of Physics and Astronomy, University of Victoria, Victoria, BC V8P 1A1, Canada

Abstract. The transverse electron scattering response function R_T of ³He is studied in the quasielastic peak region for momentum transfers between 500 and 700 MeV/c. The calculation is carried out in the active nucleon Breit frame. The response in the laboratory frame is then obtained via a transformation of R_T from the active nucleon Breit frame to the laboratory frame. For the current operator one- and two-body parts are taken into account. The one-body current operator includes all leading order relativistic corrections. For the two-body part meson exchange currents consistent with the employed NN potential (Argonne V18) are taken. As three-nucleon force the Urbana IX model is used. In comparison with experiment one finds an excellent agreement of the peak positions. The peak height agrees well with experiment for the lowest considered momentum transfer (500 MeV/c), but tends to be too high for higher momentum transfer (10% at 700 MeV/c).

1 Introduction

The transverse quasielastic response function $R_T(q, \omega)$ of nuclei is dominated by the one-body part of the nuclear current. With increasing momentum transfer q relativistic effects become more and more important. In fact at $q = 500$ MeV/c one finds a considerable disagreement for ³He between experimental data and non-relativistic theoretical calculations [1–3]. In particular there is a significant mismatch of experimental and theoretical quasielastic peak positions. Similar discrepancies were also found for the longitudinal response function $R_L(q, \omega)$ of the three-nucleon systems. The discrepancies between theory and experiment persisted even when leading order relativistic effects were included in the nuclear charge operator [4]. On the other hand it was shown in [5] that a much better agreement of theory and experiment can be obtained by an improved consideration of relativistic effects due to a calculation of the response in the active nucleon Breit (ANB) frame.

In the ANB frame the target nucleus moves with momentum $\mathbf{P}_i = -A\mathbf{q}/2$. Considering the quasielastic mechanism, *i.e.* energy and momentum transfer ω and q are picked up by a single nucleon which then escapes from the nucleus, one has the following situation: in the initial nuclear state nucleons are moving approximately with momenta $-\mathbf{q}/2$, while in the final state the knocked-out nucleon is moving with momentum $\mathbf{q}/2$. Thus in the ANB frame the energy transfer ω is equal to zero. This has to be compared with the laboratory (lab) frame case: in the initial nuclear state nucleons are moving approximately with

momenta zero and in the final state the knocked-out nucleon is moving with momentum \mathbf{q} and thus $\omega = T_N = (q^2 + M^2)^{1/2} - M$, where M is the nucleon mass and T_N denotes the kinetic energy of the outgoing nucleon. One sees (i) that the nucleons in the ANB frame are less relativistic and (ii) that in a non-relativistic lab frame description the kinetic energy T_N of the knocked-out nucleon becomes problematic for momentum transfers greater or equal about 500 MeV/c. Indeed at $q = 500$ MeV/c one has $T_N = 125$ MeV, whereas the non-relativistic kinetic energy $T_N^{\text{nonrel}} = q^2/(2M)$ corresponds to 133 MeV. This difference leads to the above mentioned mismatch of the theoretical and experimental quasielastic peak positions. This was also nicely confirmed in [5], where $R_L(q, \omega)$ was calculated for various different reference frames considering the full final state interaction but adopting the quasielastic picture for the treatment of the kinetic energy. In fact it was assumed that the whole energy transfer ω goes into the relative kinetic energy of knocked-out nucleon and residual nucleus and in addition the correct relativistic relative momentum was taken. Comparing, after a proper transformation, the various results in the lab frame the same peak positions were obtained in all cases, whereas a non-relativistic treatment leads to different peak positions. It is important to note that only for the ANB frame relativistic and non-relativistic peak positions coincide. This nice property of the ANB frame is due to the fact that ω_{ANB} is equal to zero at the quasielastic peak.

^a e-mail: leideman@science.unitn.it

2 Formalism

The transverse electron scattering response function may be written as

$$R_T(q, \omega) = \frac{1}{2J_i + 1} \sum_{M_i} \sum_{\bar{f}} df(\mathbf{J}_i^\dagger)_{i\bar{f}} \cdot (\mathbf{J}_i)_{\bar{f}i} \delta(E_{\bar{f}} - E_i - \omega).$$

Here the subscripts i and \bar{f} label, respectively, an initial state and final states, including their total momenta \mathbf{P}_i and $\mathbf{P}_{\bar{f}}$. One may write $d\bar{f} = d\mathbf{P}_{\bar{f}} df$. The above equation contains df only. The notation $E_i, E_{\bar{f}}$ refers to total initial and final-state energies, while J_i and M_i denote total angular momentum and magnetic quantum number of the initial state. The quantities $(\mathbf{J}_i)_{\bar{f}i}$ are on-shell matrix elements of the transverse component of the nuclear current operator $\bar{\mathbf{J}}(\mathbf{q}, \omega)$,

$$(\mathbf{J}_i)_{\bar{f}i} \delta(\mathbf{P}_{\bar{f}} - \mathbf{P}_i - \mathbf{q}) = \langle \Psi_{\bar{f}} | \bar{\mathbf{J}}_i(\mathbf{q}, \omega) | \Psi_i \rangle.$$

The response function $R_T(q, \omega)$ is calculated using the Lorentz integral transform (LIT) method [6], *i.e.* an integral transform of $R_T(q, \omega)$ with a Lorentzian kernel is evaluated at $q = \text{const}$:

$$L(\sigma_R, \sigma_I) = \int d\omega \frac{R_T(q = \text{const}, \omega)}{(\omega - \sigma_R)^2 + \sigma_I^2}.$$

In the LIT method the full final state interaction is taken into account, but different from conventional approaches, a calculation of continuum state wave functions is not necessary. In fact the scattering state problem is reduced to a bound-state like problem, namely to the LIT equation

$$(H - E_i - \sigma_R - i\sigma_I) |\tilde{\Psi}\rangle = \bar{\mathbf{J}}_i |\Psi_i\rangle,$$

where H is the nuclear Hamiltonian. The solution $\tilde{\Psi}$ leads to the above integral transform:

$$L(\sigma_R, \sigma_I) = \langle \tilde{\Psi} | \tilde{\Psi} \rangle.$$

In a final step $L(\sigma_R, \sigma_I)$ is inverted [7–9] in order to determine $R_T(q = \text{const}, \omega)$. More details about the LIT approach are given in a rather recent review article [10].

In the present work we take the Argonne V18 (AV18) NN potential and the UrbanaIX (UIX) three-nucleon force as nuclear force model. Bound state and LIT equations are solved using expansions in correlated hyperspherical harmonics [10].

The nuclear one-body current $\mathbf{J}^{(1)}$ consists of the non-relativistic current plus all the relativistic corrections up to order M^{-2} *i.e.* it includes the spin and convection current terms which are of order M^{-1} plus all the terms of order M^{-3} leading to

$$\mathbf{J}^{(1)}(\mathbf{q}, \omega, P_i) = \mathbf{j}_{spin} + \mathbf{j}_p + \mathbf{j}_q + \Delta\mathbf{j} + (\omega/M)\mathbf{j}_\omega,$$

with

$$\mathbf{j}_{spin} = e^{i\mathbf{q}\mathbf{r}'} \frac{i[\boldsymbol{\sigma} \times \mathbf{q}]}{2M} \left[G_M \left(1 - \frac{q^2}{8M^2} \right) - G_E \frac{\kappa^2 q^2}{8M^2} \right],$$

$$\begin{aligned} \mathbf{j}_p &= e^{i\mathbf{q}\mathbf{r}'} \frac{\mathbf{p}'}{M} \left\{ G_E \left[1 - \frac{q^2}{8M^2} (\kappa^2 + 2) \right] + G_M \frac{q^2}{8M^2} \right\}, \\ \mathbf{j}_q &= e^{i\mathbf{q}\mathbf{r}'} \frac{\kappa\mathbf{q}}{2M} \left\{ G_E \left[1 - \frac{q^2}{8M^2} (\kappa^2 + 3) \right] + G_M \frac{q^2}{4M^2} \right\}, \\ \Delta\mathbf{j} &= \frac{e^{i\mathbf{q}\mathbf{r}'}}{8M^3} \left\{ -2G_E \left[\kappa\mathbf{q}(p')^2 + 2\mathbf{p}'(p')^2 + 2\kappa\mathbf{p}'(\mathbf{p}' \cdot \mathbf{q}) \right] \right. \\ &\quad \left. + \left[G_M - G_E(1 + 2\kappa^2) \right] \mathbf{q}(\mathbf{p}' \cdot \mathbf{q}) \right. \\ &\quad \left. - 2iG_E[\boldsymbol{\sigma} \times \mathbf{q}] \left[(p')^2 + \kappa(\mathbf{p}' \cdot \mathbf{q}) \right] \right. \\ &\quad \left. + i(G_E - G_M)[\mathbf{p}' \times \mathbf{q}] \left[\kappa(\boldsymbol{\sigma} \cdot \mathbf{q}) + 2(\boldsymbol{\sigma} \cdot \mathbf{p}') \right] \right\}, \end{aligned}$$

and

$$\mathbf{j}_\omega = e^{i\mathbf{q}\mathbf{r}'} \frac{G_E - 2G_M}{8M} (\mathbf{q} + i\kappa[\boldsymbol{\sigma} \times \mathbf{q}] + 2i[\boldsymbol{\sigma} \times \mathbf{p}']).$$

We use the notation $\mathbf{r}' = \mathbf{r} - \mathbf{R}$ and $\mathbf{p}' = \mathbf{p} - A^{-1}\mathbf{P}$, \mathbf{P} and \mathbf{R} being the total momentum operator and the non-relativistic center of mass operator. In the above expressions $G_{E,M}$ are the usual nucleon form factors and

$$\kappa = 1 + \frac{2P_i}{Aq}.$$

We have calculated the above current operator from the expression for the corresponding single-particle matrix element of the form $\langle \mathbf{p}_f | \mathbf{J} | \mathbf{p}_i \rangle$ given in [11]. For more details concerning the one-body operator see [12].

For the two-body current $\mathbf{J}^{(2)}$ we take a generalized π - and ρ -exchange current consistent with the AV18 potential [13] (see also the contribution of Tomusiak et al. in this volume).

After having determined the response functions in the ANB frame they are transformed to the lab frame according to

$$R_T(q_{\text{lab}}, \omega_{\text{lab}}) = \frac{E_i^{\text{ANB}}}{M_T} R_T^{\text{ANB}}(q_{\text{ANB}}, \omega_{\text{ANB}}). \quad (1)$$

Here M_T is the mass of the target.

3 Results and Discussion

The calculation of $R_T^{\text{ANB}}(q_{\text{ANB}}, \omega_{\text{ANB}})$ is carried out for 8 different momentum transfers q_{ANB} : 400, 450, 500, 550, 600, 650, 700, and 750 MeV/c. This enables us to determine $R_T(q_{\text{lab}}, \omega_{\text{lab}})$ at $q_{\text{lab}}=500, 600, \text{ and } 700$ MeV/c (for further details see [12]). We perform a multipole expansion of the transverse current operator and consider electric and magnetic multipole contributions up to a maximal total angular momentum J_f^{max} of the final state such that a convergent result of R_T is obtained for any q value. For instance we take $J_f^{\text{max}} = 19/2$ and $37/2$ for $q = 400$ and $q = 750$ MeV/c, respectively. For the LIT parameter σ_I we choose two different values, namely $\sigma_{I,1} = 5$ MeV and

$\sigma_{I,2} = 50$ MeV, and combine both cases to a single integral transform:

$$L_{\text{tot}}(\sigma_R, \sigma_I) = L(\sigma_R, \sigma_{I,1})f(\sigma_R) + \left(\frac{\sigma_{I,2}}{\sigma_{I,1}}\right)^2 L(\sigma_R, \sigma_{I,2})(1 - f(\sigma_R)),$$

where

$$f(\sigma_R) = \exp(-(\sigma_R/\sigma_0)^6) \quad (\sigma_R \geq 0), \quad f(\sigma_R) = 1 \quad (\sigma_R \leq 0)$$

with $\sigma_0 = 100$ MeV. This choice has the advantage that one has a relatively large resolution for the R_T behavior at lower energies, whereas for the high-energy behavior a smaller resolution is completely sufficient. The integral equation that corresponds to the transform L_{tot} has been inverted in order to determine R_T , where the inversion of the LIT [7–9] has been made as described in [3].

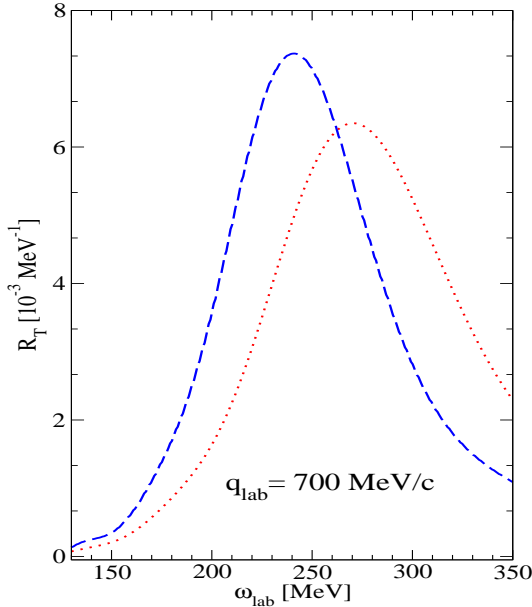


Fig. 1. $R_T(q_{\text{lab}}, \omega_{\text{lab}})$ of ${}^3\text{He}$ at $q_{\text{lab}} = 700$ MeV/c from ANB (dashed) and lab (dotted) frame calculations with non-relativistic one-body current.

In Fig. 1 we show $R_T(q_{\text{lab}} = 700 \text{ MeV/c}, \omega_{\text{lab}})$ calculated in the ANB frame, then transformed to the lab frame with Eq. (1), taking as nuclear current operator the non-relativistic one-body current only. In comparison we illustrate the corresponding R_T from the lab frame calculation. The two results exhibit rather different peak positions. As pointed out in the introduction, the lab frame calculation should lead to a peak at about $\omega_{\text{lab}} = q_{\text{lab}}^2/(2M) = 261$ MeV, while in case of the ANB frame one expects the peak at about $\omega_{\text{lab}} = (q_{\text{lab}}^2 + M^2)^{1/2} - M = 232$ MeV. Thus one should have a difference for both peak positions of about 30 MeV. In fact in Fig. 1 such a difference can be observed, but the actual peak positions are shifted both by about 10 MeV towards higher energy. This shift is explained by the fact that our calculation does not correspond

to a simple quasielastic treatment. Indeed the full many-body final state interaction is rigorously taken into account in our calculation.

In Fig. 1 one also notes differences for the peak heights: the peak of the ANB frame calculation is 15% higher than the peak of the lab frame calculation.

For the two other considered momentum transfers, not shown here, we find smaller shifts for the peak positions (9 MeV at $q = 500$ MeV/c, 17 MeV at $q = 600$ MeV/c) and less overestimation of the peak heights (5% at $q = 500$ MeV/c, 10% at $q = 600$ MeV/c). For more details see [12].

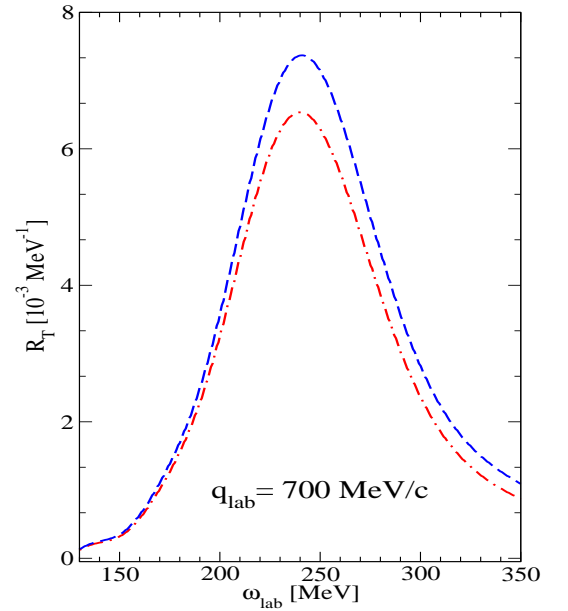


Fig. 2. $R_T(q_{\text{lab}}, \omega_{\text{lab}})$ of ${}^3\text{He}$ at $q_{\text{lab}} = 700$ MeV/c from ANB frame calculation with relativistic (dash-dotted) and non-relativistic (dashed) one-body current.

In Fig. 2 we show the effect of the leading order relativistic corrections to the one-body nuclear current operator at $q_{\text{lab}}=700$ MeV/c. They lead to a reduction of the transverse response function in the whole considered energy range. In the peak the decrease amounts to 11%. For the here not shown cases of $q = 500$ and 600 MeV/c one has reductions of 6% and 8%, respectively (see [12]).

A further inclusion of meson exchange currents has only a rather small impact on the result. In [12] we find the following increases of the quasielastic peak heights: 3.2% (500 MeV/c), 2.7% (600 MeV/c), and 2.2% (700 MeV/c). These rather small effects do not come as a surprise, since, as we have already pointed out, the quasielastic region is dominated by a one-body knock-out.

A comparison of our results with experimental data is displayed in Fig. 3 at $q_{\text{lab}} = 500, 600,$ and 700 MeV/c. It is evident that there is an excellent agreement of experimental and theoretical peak positions for all the three cases. For the peak heights one finds a somewhat different scenario. There is a very good agreement at $q_{\text{lab}} = 500$ MeV/c, a slight overestimation of experiment by theory of about 5% at $q_{\text{lab}} = 600$ MeV/c, which increases to an overestima-

tion of about 10% at $q_{\text{lab}} = 700$ MeV/c. Most probable the growing differences of theoretical and experimental results have to be attributed to not considered relativistic effects in the calculation.

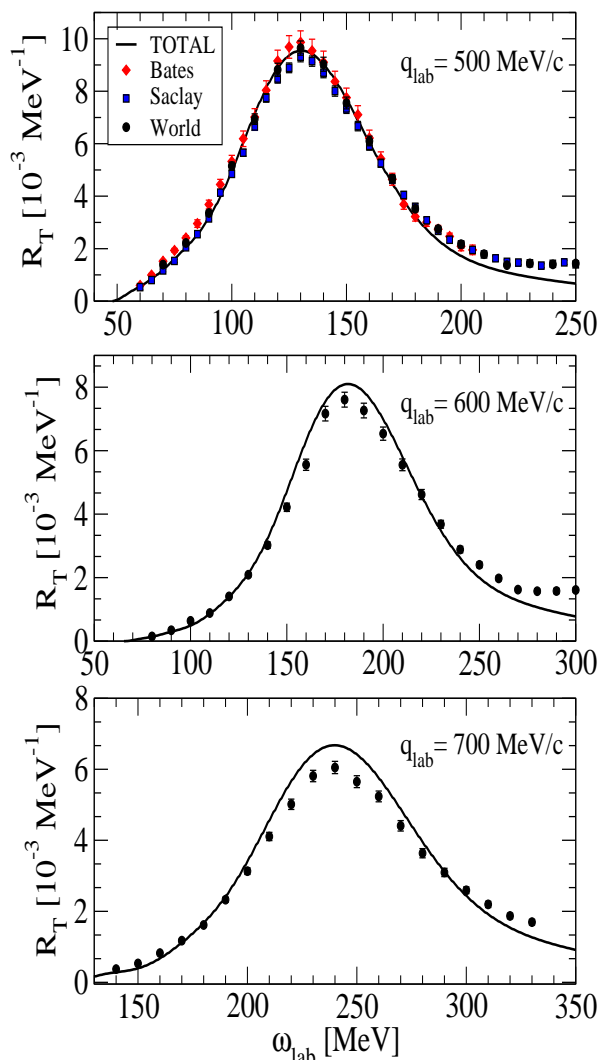


Fig. 3. $R_T(q_{\text{lab}}, \omega_{\text{lab}})$ of ^3He from ANB frame calculation with relativistic one-body and meson exchange current (full) in comparison to experimental results from [14] (squares), [15] (diamonds), [16] (circles).

Different from the experimental R_T , our theoretical R_T does not contain the pion production channel. In this respect it is interesting to note that the deviation of experimental and theoretical results at $q_{\text{lab}} = 500$ MeV/c sets in just at pion production threshold, which is equal to about 180 MeV for this momentum transfer.

To sum up we can say the following. We have calculated the ^3He transverse response function $R_T(q, \omega)$ with a realistic nuclear force (AV18 two-nucleon and UIX three-nucleon potential) in the quasi-elastic region at $500 \text{ MeV/c} \leq q \leq 700 \text{ MeV/c}$ with full inclusion of final state interaction. The calculation is carried out in the ANB frame with a subsequent transformation of R_T to the lab system. Rel-

ativistic effects to the one-body current operator as well as meson exchange currents are taken into account. The relativistic effects reduce the quasi-elastic peak, while the MEC contributions are rather unimportant. The use of the ANB frame provides excellent agreement with experimental peak positions. Concerning the peak heights one finds a good agreement of theoretical and experimental results at $q = 500$ MeV/c, while theory overestimates data up to 10% at higher q .

References

1. A. Deltuva, L.P. Yuan, J. Adam Jr, and P.U. Sauer, Phys. Rev. **C70**, (2004) 034004
2. J. Golak, R. Skibinski, H. Witala, W. Glöckle, A. Nogga, and H. Kamada, Phys. Rep. **415**, (2005) 89
3. S. Della Monaca, V.D. Efros, A. Khugaev, W. Leidemann, G. Orlandini, E.L. Tomusiak, and L. P. Yuan, Phys. Rev. **C77**, (2008) 044007
4. V.D. Efros, W. Leidemann, G. Orlandini, and E.L. Tomusiak, Phys. Rev. **C69**, (2004) 044001
5. V.D. Efros, W. Leidemann, G. Orlandini, and E.L. Tomusiak, Phys. Rev. **C72**, (2005) 011002(R)
6. V.D. Efros, W. Leidemann, and G. Orlandini, Phys. Lett. **B338**, (1994) 130
7. V.D. Efros, W. Leidemann, and G. Orlandini, Few-Body Syst. **26**, (1999) 251
8. D. Andreasi, W. Leidemann, Ch. Reiss, and M. Schwamb, Eur. Phys. J. **A24**, (2005) 361
9. N. Barnea, V.D. Efros, W. Leidemann, and G. Orlandini, *arXiv:0906.5421*.
10. V.D. Efros, W. Leidemann, G. Orlandini, and N. Barnea, J. Phys. **G34**, (2007) R459
11. F. Ritz, H. Göller, T. Wilbois, and H. Arenhövel, Phys. Rev. **C55**, (1997) 002214
12. V.D. Efros, W. Leidemann, G. Orlandini, and E.L. Tomusiak, *arXiv:0910.2406*
13. W. Leidemann, V.D. Efros, G. Orlandini, and E.L. Tomusiak, *arXiv:0906.0663*, Few-Body Syst. in print, DOI 10.1007/s00601-009-0078-8
14. C. Marchand *et al.*, Phys. Lett. **B153**, (1985) 29
15. K. Dow *et al.*, Phys. Rev. Lett. **61**, (1988) 1706
16. J. Carlson, J. Jourdan, R. Schiavilla, and I. Sick, Phys. Rev. **C65**, (2002) 024002